Materials Research Proceedings 28 (2023) 1897-1906 https://doi.org/10.21741/9781644902479-205

Experimental measurement of CF/PEKK tapes heating behavior in the laser assisted automated fiber placement process

LE LOUËT Violaine[1,a], LE REUN Adrien[2,b], SOBOTKA Vincent[2,c *] and LE CORRE Steven[2,d]

[1]CAPACITES SAS, 26 bd Vincent Gâche F-44200 Nantes, France

[2]Nantes Université, CNRS, LTEN, UMR 6607, F-44000 Nantes, France

[a]Violaine.Le-louet@univ-nantes.fr, [b]adrien.le-reun@univ-nantes.fr, [c]vincent.sobotka@univ-nantes.fr, [d]steven.lecorre@univ-nantes.fr

Keywords: Heat Transfer, Infrared Camera, Automated Fiber Placement

Abstract. This work takes place within the framework of the study and control of heat transfer taking place during the heating stage of the Laser Assisted Automated Fiber Placement (AFP) process. Understanding the interaction between the composite tape and the incoming laser radiation is a cornerstone for controlling the thermal history of the laminate. Laser incidence, fibre orientation and lay-up velocity have long been identified as key factors influencing the laser absorption by the composite and its increase in temperature. For the sake of simplicity, homogenous model is often used to describe phenomena inside the composite. However, the study of the radiative behaviour of laminates and tapes has shown that absorption occurs over a volume whose size depends on the carbon fibre architecture within the polymer matrix. Investigating heat transfer at micro scale is then crucial to fully understand the thermal phenomena occurring in the AFP process. In order to investigate heat transfer according to process parameters and especially to the orientation of the tape, a specific bench is developed in order to perform static heating a single composite with a laser diode. A full calibration of the bench was first performed including the response of the IR camera as well as the shape and power imposed by the laser source. Then, measurements for several orientations of the tape (0°,45° and 90°) were performed and thermal response measured and analysed.

Introduction

From their potential recyclability, bonding ability and tenacity in comparison with thermoset, the interest for thermoplastic composites steeply increased for years. Development of technical polymers with melting temperatures reaching 400°C made conceivable their use in structural parts, especially in aeronautics.

Among the manufacturing processes, Automated Fibre Placement (AFP) processes have been pointed out as suitable solutions to meet these expectations [1,2]. This process is based on the laying of narrow prepreg tapes with automated systems. The laser-assisted thermoplastic AFP process is promising to enable complex shapes manufacturing and in-situ consolidation. The process is simplified with three steps which are depicted in Fig. 1: heating, adhesion and consolidation phases. First, the laying tape and the substrate are heated such as both reach the matrix melting temperature. Heating phase must ensure that ply and substrate temperatures reach the matrix melting temperature without exceeding the matrix degradation temperature [3-5]. Then, the compaction roller pressurizes the ply (laying tape) and the substrate to increase intimate contact. Pressure and melting of the matrix enable bonding of ply and substrate with the inter-diffusion of polymer chains through the interface, called reptation [6]. Adhesion phase tries to maximize the degree of intimate contact [7,8] between ply and substrate based on pressure of the roller. Finally, the consolidation during cooling phase is an essential step to improve the

mechanical resistance through matrix crystallization. These statements make the prediction and modeling of heat transfers necessary steps to master the process under varying configurations: laying speed, materials properties, shape geometry, etc…

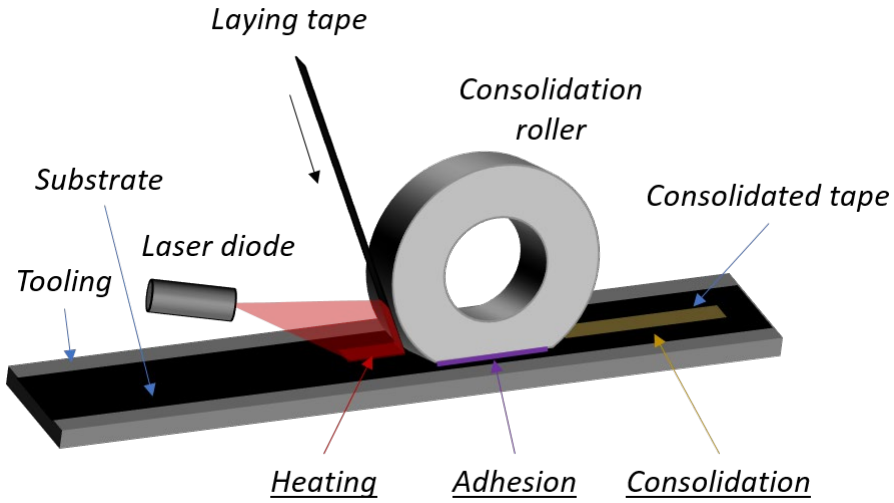

Fig. 1. Laser-assisted AFP process: heating, adhesion and consolidation.

In this article, we propose the development of an original bench representative of an AFP process enabling the precise measurement of a composite tape surface temperature heated by laser. The bench is specifically designed to study the effect of laser incidence angle and fibre orientation. Finally, a comparison with a novel numerical model is presented and discussed.

Material

The studied material is an AS7 carbon fibre [9] reinforced UD prepreg tape with a PEKK7002 [10] matrix. Fibres and matrix properties have been either extracted from datasheet, as density, considered constant in this study, or measured at laboratory with DSC for specific heat capacity and guarded hot plate for thermal conductivity.

A model of fibre conductivity with a weak transverse thermal conductivity (0.5 $W.m^{-1}.K^{-1}$) at core and a higher one on the edge (8.7 $W.m^{-1}.K^{-1}$) has been designed to account for the fibre thermal behavior. The skin thermal conductivity has been identified using the guarded hot plate measurement and a steady microstructure simulation.

Table 1. PEKK7002 and AS7 carbon fibre properties.

	PEKK7002	Carbon fibre AS7
Density ρ [kg/m^{-3}]	1290	1790
Thermal conductivity k [$W/m^{-1}/K^{-1}$]	0.27	Longitudinal: 10 Transverse (core): 0.5 Transverse (skin): 8.7
Specific heat capacity C_p [$J/kg^{-1}/K^{-1}$]	T ≤ 162°C, 3.35 T + 1017.0 162 < T < 334°C, 3.45 T + 1137.6	-0.00295 T(°C)² + 3.493 T(°C) + 578.4

Experimental Setup

In order to remove the instrumentation constraints of the dynamic process, an experimental apparatus is developed to measure the evolution of physical values during laser-heating of a single tape, such as surface temperature and heat flux between tape and tooling.

The system is developed to facilitate unidimensional heat transfer through the tape thickness. It consists of two identical frames made of steel Z35CD17 (AFNOR), whose dimensions 100x20x6 mm, maintained in contact in the plane (O,y,z). Three thermocouples are placed along the central axis at respectively 250 µm, 1.25 mm and 3.25 mm from the surface and form a flux sensor which measures heat transfer between composite and tooling (Fig. 2). This sensor is also used to calibrate the laser heat flux. In both frames, respectively 11 and 10 type K 250 µm diameter thermocouples are placed at 250 µm from the surface to measure 2D heat transfer phenomena. The lower part of the system can be heated up to 400°C thanks to heating cartridges.

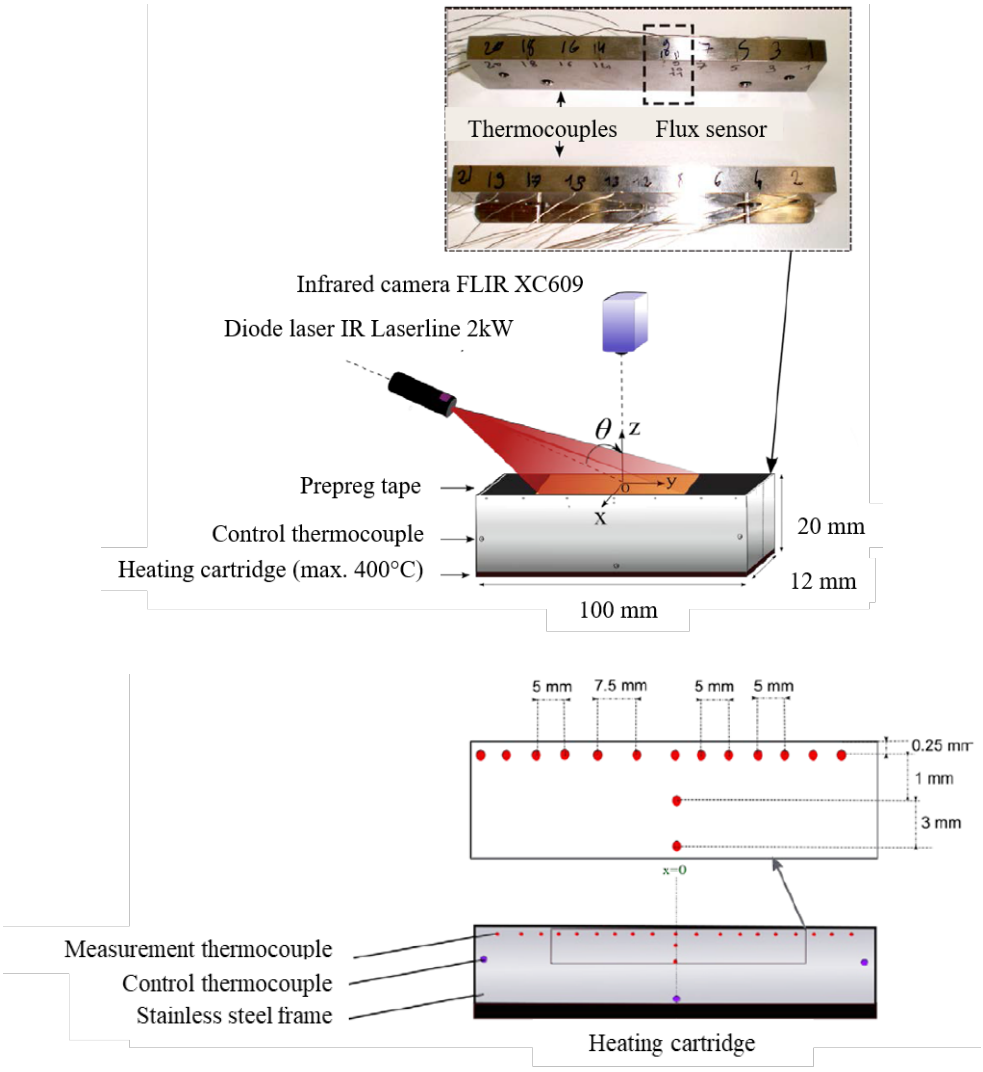

Fig. 2. Thermocouples positioning and flux sensor.

A FLIR XC609 infrared camera (Fig. 3) is maintained perpendicularly to the frame thanks to a metal support whose position is adjustable in the three axes (x,y,z) such as surface temperature is monitored in the plane (O,x,y). Heating of the tape is supplied with a laser diode LDM 2000-30 from Laserline with a maximal output power of 2000 W and of wavelength of 980 nm. The laser is mounted on a rotating arm which enables the adjustment of laser incidence angle from 0° to 70°

with respect to plane (O,x,y) and distance to tape from 150 to 200 mm. Due to bulk issues, the minimal incidence angle is 10° when camera and diode are both installed.

The tape is 12 mm wide, 60 mm long, 0.2mm thick and maintained at the tooling surface thanks to 50 N magnets. For safety issues, the whole system is installed within an opaque box.

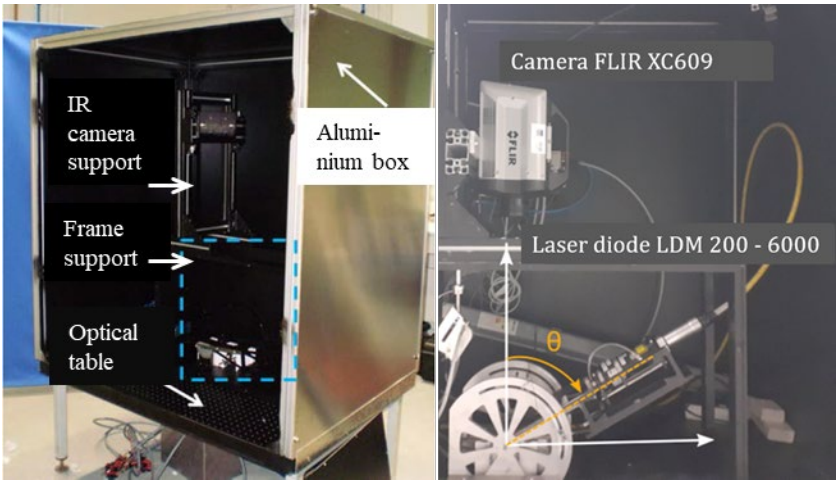

Fig. 3. Experimental apparatus.

Caracterisation of Laser Source in Normal Incidence

The laser spot is a 12x12 mm² square on which intensity is distributed in a top hat shape with a homogeneous and maximal value over a 6x6 mm² area and decreases exponentially on the edges. The nominal intensity, meaning the intensity in the central area is calibrated with the help of the heat flux sensor implemented in the metallic support. The evolution with time of an incoming heat flux irradiating the sensor surface is calculated with the Beck inverse method [11] supplied with the thermocouples responses. The usual algorithm was modified to retrieve the thermocouples response time.

During the campaign, the IR camera is removed so the laser diode can be positioned normally to surface (0°). A graphite coating of known emissivity is sprayed homogenously over the support surface. The thermal resistance of the layer is neglected as its thickness does not exceed a few dozen microns.

Calibration consisted in irradiating the surface during 100 ms at the minimum power of the laser diode. The distance with the surface was varied from 150 mm to 200 mm. Fig. 4 displays the evolution versus time of the heat flux density calculated using Beck algorithm. Overshoots can be observed at the beginning and end of irradiation. These are induced by the algorithm itself. Although its use benefits from making no assumption of the flux behaviour with time, the algorithm lacks accuracy for the identification of Heaviside functions with infinite first derivatives. The actual heat flux evolution with time is indicated with dotted lines on the graph.

The laser beam is slightly divergent and the heat flux density decreases with the distance from the surface. This evolution is linear with distance as displayed in Fig. 5.

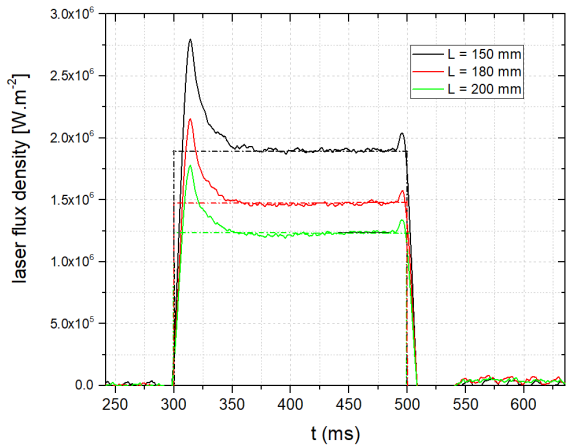

Fig. 4. Measurement of the heat flux density with time during a 100 ms pulse.

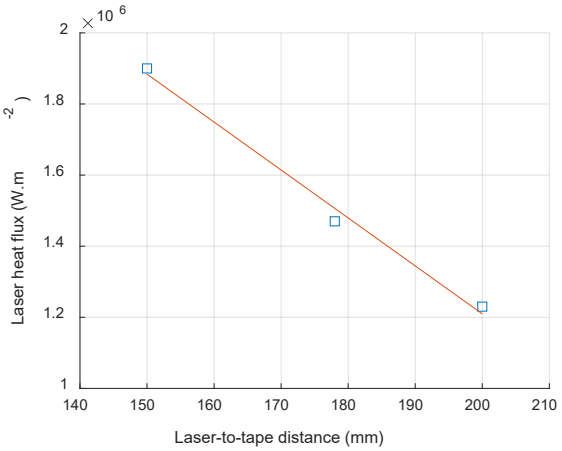

Fig. 5. Evolution of heat flux density with distance.

Tape Surface Temperature: Effect of Fibre Orientation and Incidence Angle

Tape surface temperature is measured regarding fibre orientation φ and laser incidence angle θ (Fig. 6). As temperature decreases with grazing incidences, the laser power density is adjusted in order to reach similar temperatures for every incidence angle and work in the same calibration range of the camera (Fig. 7).

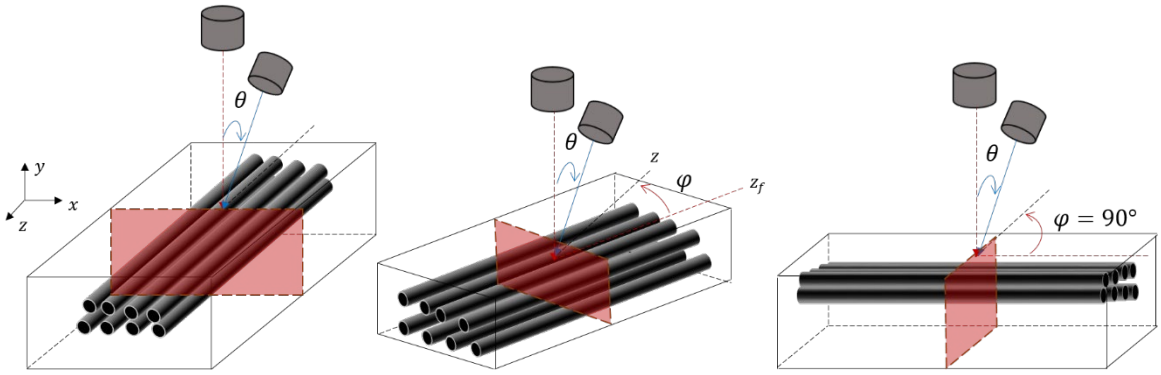

Fig. 6. Angles configuration: fibre orientation φ, incidence angle θ.

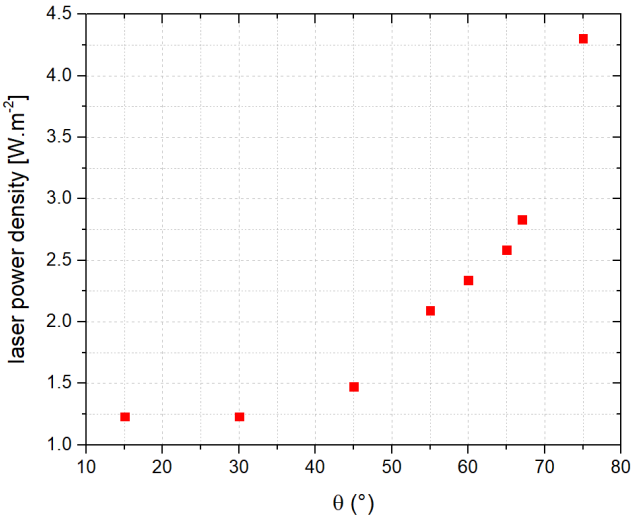

Fig. 7. Power density according to the incidence angle.

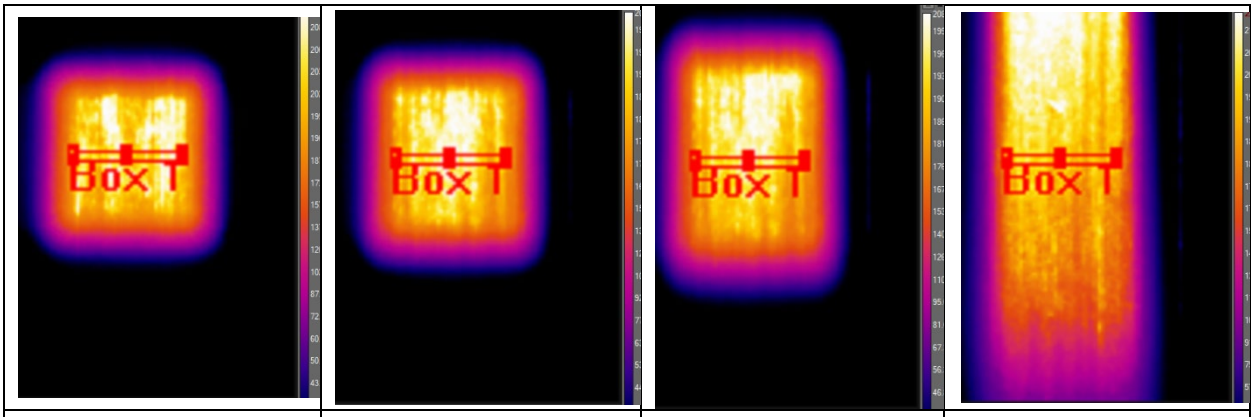

(a) θ = 15°	(b) θ = 30°	(c) θ = 45°	(d) θ = 75°

Fig. 8. Thermographs at φ = 0°.

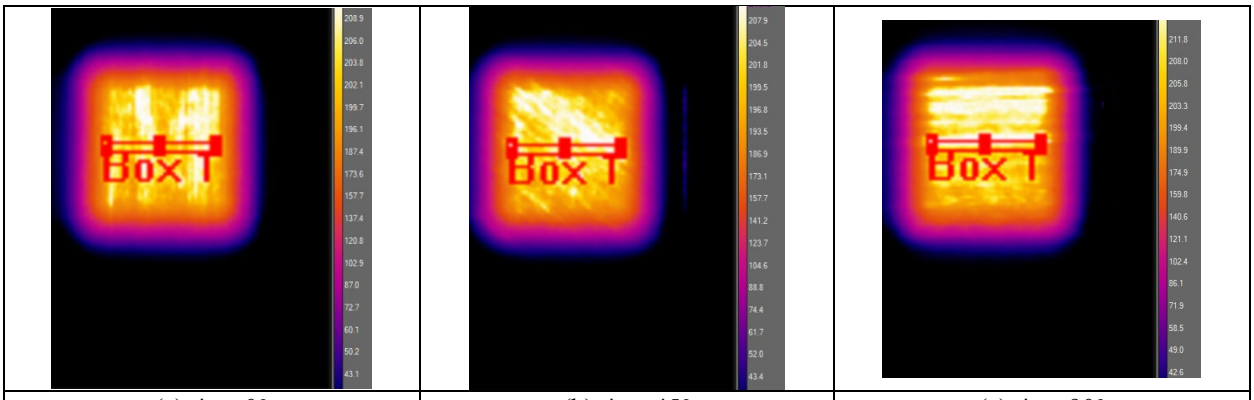

(a) ϕ = 0°	(b) ϕ = 45°	(c) ϕ = 90°

Fig. 9. Thermographs at θ = 15°.

Fig. 8 displays the thermographs at end of heating t = 20 ms for trials on a tape positioned at φ = 0° and for increasing incidence angles θ. The expansion of the laser spot length with incidence is clearly noticeable. The temperature distribution over the irradiated surface also become less homogeneous as the incidence angle decreases. As a result, temperature is extracted and averaged over a slim area (represented by the red box) aligned with pivot point of the laser diode and where

the magnitude of the laser flux has been calibrated. Similarly, thermographs are presented for three fibre orientations: 0, 45 and 90° in near-normal incidence θ = 15 (Fig. 9). The temperature variability is noticeable and due to tape heterogeneity. The color contrast highlights the fibre orientation.

Series of 5 samples have been tested in the configurations φ = 0°, 45° and 90°, and θ = 15°, 45° and 60° on which the average temperature and standard deviation are determined. The measurement uncertainty u is estimated following:

$$u = \sqrt{u(T_{mean})^2 + u(\sigma_{mean})^2} \quad (1)$$

with:

$$u(T_{mean}) = \frac{1}{\sqrt{5}}\sqrt{\frac{1}{n}\sum_{i=1}^{n=5}(T_i - T_{mean})^2} \quad (2)$$

$$u(\sigma_{mean}) = \frac{1}{\sqrt{5}}\sqrt{\frac{1}{n}\sum_{i=1}^{n=5}(T_i - \sigma_{mean})^2} \quad (3)$$

The measurement uncertainty is caused by:

1. The resolution of the camera
2. The heterogeneity of the tape surface
3. The variability of the tape over the batch
4. The variability of the test and of the operator

Results are summarized in Fig. 10. Surface temperature increases during the 20 ms heating time to reach approximately 200°C for every incidence angle. The effect of fibre orientation on the surface temperature is shown negligible as temperature differences between various fibre orientations samples are inferior to the measurement uncertainty. These experimental temperatures are compared with a novel thermo-optical model at the microscale.

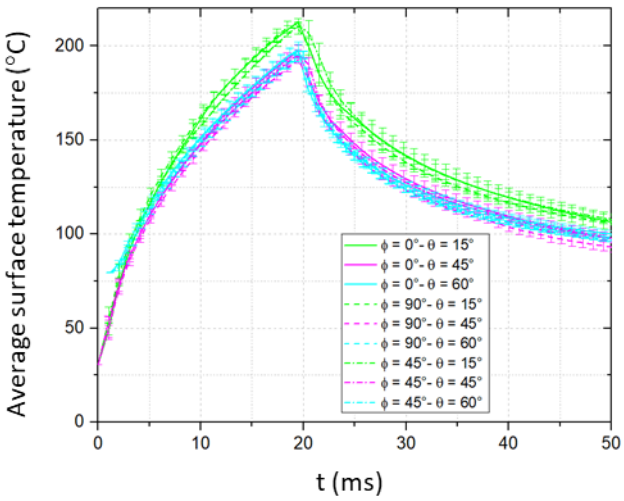

Fig. 10. Evolution of surface temperature as a function of fibre orientation (0, 45, 90°) and incidence angle (15, 45, 60°).

Numerical Model

A numerical thermo-optical model is designed at the micro-scale based on the tape microstructure. A cross-section micrograph (Fig. 11) of the experimental samples is performed and used to characterize the fibre distribution through the thickness. Image points out the heterogeneity of fibre distribution in the thickness with denser area close to the surfaces and a weaker fibre fraction at core.

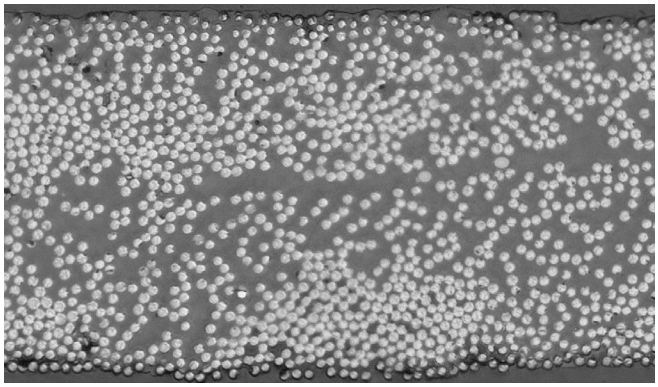

Fig. 11. Cross section micrograph of the tape.

An artificial microstructure is created based on the actual fibre distribution and used to perform a FEM simulation computed with Freefem++ [12].The matrix is considered fully transparent at the laser wavelength. [13]. Therefore, the laser beam is only absorbed by carbon fibres. A ray-tracing algorithm is developed to compute fibres areas heated by the laser beam (Fig.12) depending on fibre orientation and incidence angle. The laser beam is modelled by approximately 4000 scanning lines which are evenly spaced by a fraction of fibre element size. The intersection between the scanning lines and fibres is computed without considering refraction in the polymer matrix. Every heated carbon fibre element is tagged for the following thermal simulation in which a heat flux condition is applied based on the laser power density ϕ_{laser} and the carbon absorption coefficient α_{carbon}.

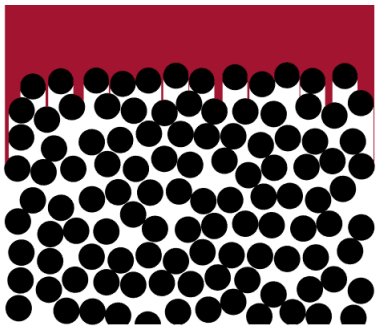

Fig. 12. Ray-tracing algorithm: detection of heated fibres by the laser beam.

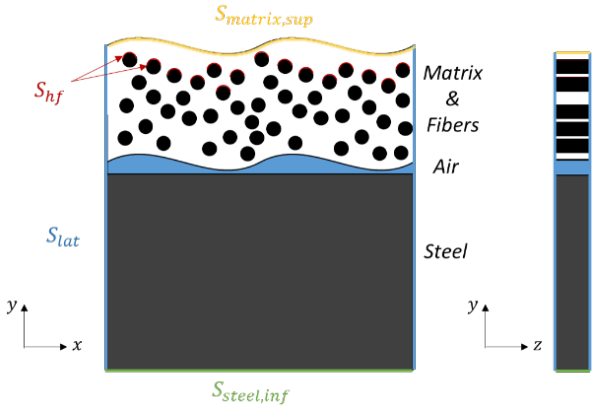

Fig. 13. Schematic of the problem: volume and boundary conditions.

The problem is modeled in Fig. 13. The heat equation is solved in the four physical volumes: fibres, matrix, steel and air.

$$\rho C_p \frac{\partial T}{\partial t} - div\left(\bar{\bar{k}} \cdot \vec{\nabla} T\right) = Q_v \quad (4)$$

with the following boundary conditions:

1. Adiabatic lateral surfaces S_{lat} (heat transfer is 1D): $\vec{\phi}.\vec{n} = 0$
2. Fixed temperature: $T = T_{amb} = 20°C$ on steel lower surface $S_{steel,inf}$
3. Dissipation by air convection on matrix upper surface $S_{matrix,sup}$: $\phi = h_{air}(T - T_{amb})$
4. Laser heat flux absorption on fibres heated elements S_{hf}: $\phi = \alpha_{carbon}\, \phi_{laser}\, \vec{q} \cdot \vec{n}$

where $h_{air} = 5$ W.m^{-2}.K^{-1} the air convection coefficient, $\alpha_{carbon} = 0.9$ the carbon absorption coefficient, $\vec{n}$ the normal vector to the element and $\vec{q}$ the resulting direction vector of laser heat flux, depending on fibre orientation and incidence angle.
The simulation is performed on 50 iterations with a 20 ms heating time which corresponds approximately to the exposure time in a manufacturing process context at a 500 mm.s^{-1} laying speed with a 12 mm laser beam width. It is also chosen to nullify the effect of back surface condition, meaning that diffusion time through the thickness is greater than 20 ms. The total time is set at 40 ms to study the cooling kinetic.

Experimental and Numerical Comparison

Average experimental and numerical surface temperatures are compared in Fig. 14 for near-normal $\theta = 15°$ and grazing $\theta = 60°$ incidences with respectively 1.31 and 2.49 MW.m^{-2} laser power density. Laser heat flux has been corrected to fit experimental and numerical temperatures.

Both incidences show an accurate approximation between experimental and numerical temperatures at the end of heating phase. The simulation confirms that fibre orientation has a negligible effect on surface temperature and the necessity to increase laser power to reach similar surface temperatures. Heating and cooling kinetics are also closed between experimental and numerical temperatures, meaning that heat transfers are rather well described by the model.

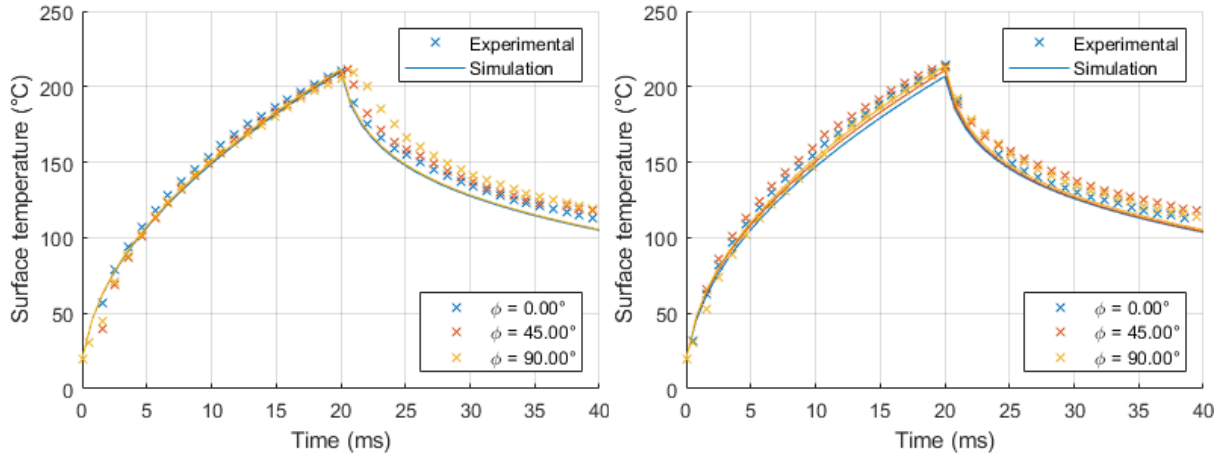

Fig. 14. Evolution of numerical and experimental surface temperature for (a) near-normal θ = 15° and (b) grazing θ = 60° incidences and three fibre orientations.

Summary
A specific experimental bench is designed to study heat transfer in the laser-heating of a single carbon fiber reinforced composite tape in a static configuration. The bench is instrumented with thermocouples and an infrared camera to measure laser heat flux and tape surface temperatures. A thermo-optical model is developed and approximates the evolution of surface temperatures. Both experimentation and simulation results highlighted the negligible effect of fibre orientation on surface temperatures. However, laser power has to be increased with grazing incidences to reach a similar surface temperature.

Acknowledgments
This work was conducted under the framework of HAICoPAS, a PSPC project (projet de recherche et développement structurant pour la compétitivité). Authors are grateful to the partners of the HAICOPAS Project (Hexcel Composites, Arkéma, Coriolis, Institut de Soudure, PEI, Ingecal) for their interest and support to this research.

References
[1] D. H.-J. Lukaszewicz, C. Ward, K.D. Potter, The engineering aspects of automated prepreg layup: History, present and future, Compos. Part B: Eng. (2012) 997-1009. https://doi.org/10.1016/j.compositesb.2011.12.003
[2] Z. August, G. Ostrander, J. Michasiow, D. Hauber, Recents developments in automated fiber placement of thermoplastic composites, Sampe J. 50 (2014) 30-37.
[3] K. Cole, I. Casella, Fourier transform infrared spectroscopic study of thermal degradation in films of poly (etheretherketone), Thermochimica acta 211 (1992) 209-228. https://doi.org/10.1016/0040-6031(92)87021-2
[4] M. Day, D. Sally, D. Wiles, Thermal degradation of poly (aryl-ether-ether-ketone): Experimental evaluation of crosslinking reactions, J. Appl. Polym. Sci. 40 (1990) 1615-1625. https://doi.org/10.1002/app.1990.070400917
[5] P. Tadini, N. Grange, K. Chetehouna, N. Gascoin, S. Senave, I. Reynaud, Thermal degradation analysis of innovative pekk-based carbon composites for high-temperature aeronautical components, Aeros. Sci. Technol. 65 (2017) 106-116. https://doi.org/10.1016/J.AST.2017.02.011
[6] P.-G. De Gennes, Reptation of a polymer chain in the presence of fixed obstacles, J. Chem. Phys. 55 (1971) 572-579. https://doi.org/10.1063/1.1675789
[7] A. Khodaei, F. Shadmehri, Intimate contact development for automated fiber placement of thermoplastic composites, Compos. Part C: Open Access 8 (2022) 100290. https://doi.org/10.1016/j.jcomc.2022.100290
[8] O. Çelik, D. Peeters, C. Dransfeld, J. Teuwen, Intimate contact development during laser assisted fiber placement: Microstructure and effect of process parameters, Compos. Part A: Appl. Sci. Manuf. 134 (2020) 105888. https://doi.org/10.1016/j.compositesa.2020.105888
[9] Hexcel, Datasheet Carbon Fibre AS7.
[10] Arkema, Datasheet Kepstan 7002.
[11] J. Beck, B. Blackwell, A. Haji-Sheikh, Comparison of some inverse heat conduction methods using experimental data, Int. J. Heat Mass Trans. 39 (1996) 3649-3657. https://doi.org/10.1016/0017-9310(96)00034-8
[12] F. Hecht, New development in freefem++, J. Numeric. Math. 20 (2012) 251-265. https://doi.org/10.1515/jnum-2012-0013
[13] M. Villar, C. Garnier, F. Chabert, V. Nassiet, D. Samélor, J. Diez, A. Sotelo, M. Madre, In-situ infrared thermography measurements to master transmission laser welding process parameters of PEKK, Optic. Laser. Eng. 106 (2018) 94-104.